Arab J Sci Eng (2015) 40:3107–3117
DOI 10.1007/s13369-015-1777-8

RESEARCH ARTICLE - CIVIL ENGINEERING

A Damage Constitutive Model for Rock Mass with Nonpersistently Closed Joints Under Uniaxial Compression

Hongyan Liu[1,2] · **Limin Zhang**[3,4]

Received: 12 October 2014 / Accepted: 13 July 2015 / Published online: 28 July 2015

Abstract As part of the rock mass, both the macroscopic flaws such as joints and the mesoscopic flaws such as microcracks affect the strength and the deformational behavior of rock mass. Existing models can either handle any one of them alone, and a model which can consider the co-effect of these two kinds of flaws on rock mass mechanical behavior is not yet available. This study focusses on rock mass with nonpersistently closed joints and establishes a new damage constitutive model for it. Firstly, the damage model for the intact rock which contains only the mesoscopic flaws is introduced. Second, the expression of the macroscopic damage variable (tensor) which can consider the joint geometrical and mechanical properties at the same time is obtained based on the energy principle and fracture theory. Third, the damage variable based on coupling the macroscopic and mesoscopic flaws is deduced based on Lemaitre strain equivalence hypothesis, and then the corresponding damage constitutive model for rock mass with nonpersistently closed joints under uniaxial compression is set up. Finally, the test data for the intact rock under uniaxial compression are adopted to validate the proposed model. A series of calculation examples verify that the proposed model is capable of presenting the effect of joint geometrical and mechanical properties on the rock mass mechanical behavior.

Keywords Rock mass with nonpersistently closed joints · A damage constitutive model · Macroscopic and mesoscopic flaws · Damage coupling · Stress intensity factor (SIF)

List of abbreviations

SIF	Stress intensity factor
CDM	Continuum damage mechanics

List of symbols

α	Joint dip angle (°)
ε	Strain
$\mathbf{\Omega}$	The second-order damage tensor
$\mathbf{\Omega^k}$	The damage tensor for the kth set of joints
$\mathbf{\Omega_{12}}$	The coupled damage tensor
τ	Shear stress (MPa)
φ	Joint internal friction angle (°)
μ	The friction coefficient of the joint face
τ_{eff}	The slide force along the joint face (MPa)
θ	The propagation angle of the wing crack at the joint tip (°)
ϕ	The persistent ratio of the nonpersistent joints
σ	Normal stress (MPa)
$\tilde{\sigma}$	The effective stress (MPa)
$\varepsilon_{12}, \varepsilon_1, \varepsilon_2, \varepsilon_0$	The strain of the rock mass samples with both macroscopic and mesoscopic flaws, with only macroscopic flaws, with only mesoscopic flaws and without any flaws, respectively
a	The joint half length (cm)

✉ Hongyan Liu
lhyan1204@126.com

1 College of Engineering and Technology, China University of Geosciences (Beijing), Beijing 100083, People's Republic of China

2 School of Engineering, Tibet University, Lasha Xizang 850000, People's Republic of China

3 Civil and Environmental Engineering School, University of Science and Technology Beijing, Beijing 100083, People's Republic of China

4 Hebei Chengde Iron and Steel Corporation, Hebei Chengde 067002, People's Republic of China

a^k	The size of the jointed area (m^2)
A	The joint area (m^2)
B	The joint depth (cm)
D	Damage
D_0	The damage along the loading direction
D_1, D_2	Macroscopic and mesoscopic damages, respectively
D_{12}	The coupled damage variable
E	Young's modulus (MPa)
$\tilde{E}_{12}$, $\tilde{E}_1$, $\tilde{E}_2$, E_0	The elastic modulus of the rock mass samples with both macroscopic and mesoscopic flaws, with only macroscopic flaws, with only mesoscopic flaws and without any flaws, respectively (MPa)
$[\mathbf{E_0}]$	The second-order elastic tensor of intact rock (MPa)
$[\mathbf{E}]$	The second-order elastic tensor jointed rock mass (MPa)
F	An elemental strength parameter or stress level
G	Young's and shear moduli of the intact rock (MPa)
$\mathbf{I}$	The second-order unit tensor
K_{I} and K_{II}	The first and second stress intensity factors (SIF) of the joint tip, respectively (MPa$\sqrt{m}$)
K_{I0}, K_{II0}	SIF of one single I and II types of joints, respectively (MPa$\sqrt{m}$)
l^*	The length variable (cm)
l	The propagation length of the wing cracks (cm)
l_0	The average space between two neighboring joints (m)
m, F_0	The distribution parameters
n	The number of all failed ones under a certain load
$\mathbf{n^k}$	The orientation vector of the joint
N_0	The number of all mesoscopic elements
N	The joint number
$P(\varepsilon)$	The percentage of damaged ones out of the total number of the microcells in the rock
U^{E}	The unit volume elastic strain energy (MN m)
V	The volume of rock mass (m^3)
Y	The emission of damaged strain energy (MN m)

1 Introduction

Engineers and geophysicists are constantly being confronted with the need to know the global deformational behavior and strength of the jointed rock mass. The difficulties arise mostly from the complexity caused by the flaws. The scale of the flaws in the jointed rock mass varies from several millimeters even less such as microcracks to several meters even larger such as joints; therefore, the jointed rock mass may exhibit behavior extending from that of an intact rock to that of a near-homogeneous highly fractured medium. For simplification in study, the joints and microcracks are called the macroscopic and mesoscopic flaws, respectively. As is known to all, these two different scale flaws affect the jointed rock mass strength and deformability. But many existing studies [1–4] on the jointed rock mass mechanical behavior only focus on the effect of the joint on rock mass and ignore that of the microcracks. Wang et al. [1,5] established a mathematic model for the rock mass with multi-sets of ubiquitous joints and an associated numerical implementation accounting for the anisotropy in strength and deformation induced by the joints. In order to account for the roughness of the discontinuities, Halakatevakis et al. [2] extended the original plane of weakness theory by imposing the nonlinear Barton–Bandis shear strength criterion for the discontinuities. Prudencio et al. [3] ran biaxial tests on rock with nonpersistent joints and found that the joint system had much effect on the rock mass fracture modes and maximum strength. Wai et al. [6] investigated the effects of joint sets and dip angles on the rock mass strength and deformation behavior by using a three-dimensional distinct element code, 3DEC. Based on the extensive experiments, a new strength criterion for jointed rock mass proposed by Ramamurthy et al. [7] is related to the compressive strength of intact rock and the joint factor J_f which is evolved to account for the number of joints per meter length, inclination of the sliding joint and the shear strength along this joint. All the existing studies indicate that the existence of joints has much effect on the rock mass strength and deformability, leading to its anisotropy. But the shortcoming in the existing studies is that they all ignore the effect of the mesoscopic flaw on the jointed rock mass mechanical behavior. The existing results [8,9] have also proved that the stochastic microcracks would cause the isotropic damage in rock mass, which caused the strength reduction and stiffness deterioration. Therefore, it is very necessary to comprehensively consider the co-effect of these two kinds of flaws on the jointed rock mass mechanical behavior. Here, the damages in jointed rock mass caused by the macroscopic and mesoscopic flaws are called the macroscopic and mesoscopic damages, respectively.

However, the macroscopic and mesoscopic damages do not independently play a role in affecting the rock mass mechanical behavior, but are in contact with each other. The macroscopic damage is produced through many complicated damage evolution processes such as initiation, propagation and bifurcation of the microcracks. But up to now, nearly none of the existing studies on rock mass damage mechanics considers the co-effect of the two kinds of damage on rock mass. For example, Kawamoto et al. [10] and Swoboda et al. [11] only considered the effect of the macroscopic flaw on the rock mass mechanical behavior and adopted the second-order damage tensor to reflect the anisotropy in rock mass caused by it, which does not consider the effect of the mesoscopic flaw in the rock blocks cut by joints. Likewise, Grady et al. [12] and Taylor et al. [13] only considered the effect of the mesoscopic flaw on the rock mass mechanical behavior and defined the damage variable as the function of the microcrack density. They did not consider the anisotropy in rock mass caused by the macroscopic cracks formed by the propagation and coalescence of the microcracks. Therefore, the above two methods do not reflect the co-effect of these two kinds of different scale flaws on the rock mass mechanical behavior.

The numerical study done by Niu et al. [14] indicates that these two kinds of damages in the rock mass have effect on its mechanical behavior, and the complex interaction will exist between them. Therefore, how to perfectly reflect the co-effect of these two kinds of flaws on the rock mass mechanical behavior is an urgent subject to solve in rock mass damage mechanics.

It can be seen from the existing study that the initial mesoscopic damage in rock will evolve into the macroscopic damage under the load. From the scale viewpoint of the damage and its identification, there is no strict limitation between the macroscopic and mesoscopic damages, they are often related to the scale of the studied object. But for convenience in engineering analysis, it is necessary to classify these two kinds of damages and then calculate their coupling effect [15].

Now the existing study on rock mesoscopic damage mechanics is often based on the statistical damage constitutive model [16,17], which is well developed. However, the study on rock mass damage constitutive model is comparatively not enough, because the most existing studies mainly adopt the damage tensor to describe the anisotropic damage in the rock mass caused by the joints [10,11], in which only the joint geometrical property such as its length and dip angle is considered, while its mechanical property such as the shear strength is not. So, it is obvious that this definition method for the damage tensor has some deficiency. Therefore, a new rock mass damage constitutive model which includes the joint geometrical and mechanical properties at the same time is proposed in this paper. Secondly, the damage variable (tensor) comprehensively considering these two kinds of flaws is set up based on Lemaitre strain equivalence hypothesis. Then the corresponding damage constitutive model for the jointed rock mass under uniaxial compression is established. Finally, the proposed model is adopted to discuss the effect of joint dip angle, joint internal friction angle and joint length on rock mass mechanical behaviors.

2 A Damage Constitutive Model for Rock with Mesoscopic Flaws

All sorts of the mesoscopic flaws in rock are randomly distributed because rock is a product of long geological history. Therefore, statistical damage mechanics is a powerful tool to study the occurrence, propagation and coalescence processes of these mesoscopic flaws and their effect on rock mechanical behaviors. By means of statistical damage mechanics, the distribution law of these mesoscopic flaws in rock such as normal or Weibull distribution is assumed so as to build up the mesoscopic elements with strength in rock and to determine its damage state. Thus, a damage statistical constitutive model for rock can be set up. Till now, much progress in the study of damage statistical constitutive models has been made [16,17]. The establishment of a rock damage statistical constitutive model is mainly based on the following two aspects: (1) choose strength criteria for the rock mesoscopic element, for instance, the maximum principle strain criterion, Mohr–Coulomb criterion and Drucker–Prager criterion; and (2) determine the distribution law of the rock mesoscopic element strength, for example power function distribution and Weibull distribution. The studies show that the damage constitutive model based on Weibull distribution is better than that based on power function distribution, and its calculation process is easier. Therefore, the damage constitutive model based on Weibull distribution and the maximum principle strain criterion is adopted here.

2.1 Establishment of the Damage Statistical Constitutive Model Based on Weibull Distribution

The strength of mesoscopic elements observes the following Weibull distribution function [18]:

$$P(F) = \begin{cases} \frac{m}{F_0}\left(\frac{F}{F_0}\right)^{m-1} \exp\left[-\left(\frac{F}{F_0}\right)^m\right] & F > 0 \\ 0 & F \leq 0 \end{cases} \quad (1)$$

where F is an elemental strength parameter or stress level, and because the strain strength theory is adopted here, it denotes strain; m and F_0 are the distribution parameters; and $P(F)$ is the percentage of damaged ones out of the total number of the microcells in the rock [8].

Let N_0 denote the number of all mesoscopic elements and n denote the number of all failed ones under a certain load. The damage D can be defined as:

$$D = \frac{n}{N_0} \quad (2)$$

where D takes a value between 0 and 1 corresponding to damage states of the rock from undamaged to fully damaged.

When the strain level ε increases to $\varepsilon + d\varepsilon$, the number of failed mesoscopic elements increases by $N_0 P(F)d\varepsilon$. If external load increases from 0 to ε, the total number of failed mesoscopic elements is:

$$n = \int_0^F N_0 P(F)\mathrm{d}F = N_0 \left\{1 \exp\left[-\left(\frac{F}{F_0}\right)^m\right]\right\} \quad (3)$$

Substituting Eq. (3) into (2) yields:

$$D = 1 - \exp\left[-\left(\frac{F}{F_0}\right)^m\right] \quad (4)$$

Equation (4) is the damage evolution equation of mesoscopic elements in the statistical constitutive model for rock.

Assuming the mechanical behavior of the rock mesoscopic elements observes Hooke law, its constitutive law is:

$$\sigma = E\varepsilon(1 - D) \quad (5)$$

where E and ε are the Young's modulus and strain for the intact rock, respectively.

2.2 Determination of Distribution Parameters

The following stress–strain relationship can be derived from Eq. (5):

$$\frac{\sigma}{E\varepsilon} = \exp\left[-\left(\frac{F}{F_0}\right)^m\right] \quad (6)$$

Equation (7) can be obtained by natural logarithm operation on both sides of Eq. (6):

$$\ln\left(-\ln\frac{\sigma}{E\varepsilon}\right) = m\ln F - m\ln F_0 \quad (7)$$

Let

$$y = \ln\left(-\ln\frac{\sigma}{E\varepsilon}\right)$$
$$x = \ln F$$
$$x_0 = -m\ln F_0$$

then

$$y = mx + x_0 \quad (8)$$

Obviously, Eq. (8) is linear, in which m is the slope of beeline and x_0 is the intercept. Parameter m and F_0 can be obtained by fitted with the test data.

3 A Damage Constitutive Model for Rock Mass with Macroscopic Flaws

Now how to describe the effect of joints on the rock mass mechanical behavior is a hot and difficult subject in rock mass mechanics. The fault in rock mass is larger and fewer and can be simulated with the joint element such as Goodman element [19] or Desai element [20]. While obviously different from it, the joint belongs to the third- and fourth-class structural face, which is small, many and nonpersistent, and it cannot be calculated one by one. Therefore, many scholars adopt the damage theory to study this problem, which regards that the existence of joints will lead to the rock mass strength reduction and stiffness deterioration. Assuming the constitutive law for the damaged rock mass still conforms to Hooke law, the effect of the joint on rock mass mechanical behavior is the deterioration of elastic modulus. So, the relationship between elastic constants and damage tensor of jointed rock mass can be expressed as follows:

$$[\mathbf{E}] = (\mathbf{I} - \mathbf{\Omega}) : [\mathbf{E}_0] \quad (9)$$

where $[\mathbf{E_0}]$ and $[\mathbf{E}]$ are the second-order elastic tensor of intact rock and jointed rock mass, respectively, $\mathbf{I}$ is a second-order unit tensor, and $\mathbf{\Omega}$ is the second-order damage tensor for the joint in the rock mass in two-dimensional problems.

Therefore, determination of the damage constitutive model for jointed rock mass is boiled down to the calculation of damage tensor. The phenomenological second-order tensor which is directly related to the geological data of the jointed rock mass is chosen as the damage tensor of continuum damage mechanics (CDM) in two-dimensional problems. Scholars have proposed many kinds of definitions of the second-order damage tensor to describe anisotropic damage of the jointed rock mass. For instance, Kawamoto et al. [10] proposed a damage model for the rock mass with a single set of joints (a series of joints parallel to each other):

$$\mathbf{\Omega^k} = \frac{l_0}{V}a^k\left(\mathbf{n^k} \otimes \mathbf{n^k}\right) \quad (10)$$

where l_0 is the average space between two neighboring joints; V is the volume of rock mass; a^k is the size of the jointed area; $\mathbf{n^k}$ is the orientation vector of the joint; and $\mathbf{\Omega^k}$ is the damage tensor for the kth set of joints.

It is often used to define the damage in rock mass geometrical damage theory [10,11,21]. But its deficiency is obvious, in which only the joint geometrical property such as its length and dip angle is considered, while its mechanical one such as its shear strength is not included in Eq. (10). That is to say, it thinks that damage cannot transfer the stress, which is nearly true to the rock mass under tension, but not to the rock mass under compression. Because the joint will close and slip along the joint face under compression, the joint can transfer part of compressive and shear stresses. The transferring coefficient is much related to the strength parameters of the joint such as its internal friction angle and cohesion. Therefore, both Kawamoto [10] and Yuan et al. [22] introduced the joint transferring compression and shear coefficients to revise the above model by considering the condition that the joint can transfer part of the compressive and shear stresses. But how to accurately define these two coefficients also becomes a new problem. However, Swoboda et al. [11] introduced the material constant $H_d (0 \leq H_d < 1)$ to consider the effect of joint contact on the stress transfer, and now the method to determine it is mainly by experience.

So, it can be seen from the existing studies that the joint property such as geometrical ones and mechanical ones is separately considered. Namely, the joint geometrical property is firstly adopted to define the damage tensor, and then its mechanical one such as its shear strength is adopted to revise the above calculation result, which not only causes inconvenience in application of this model but also is difficult to use in engineering because of the arbitrariness in selecting these parameters. Can a damage tensor which includes both the joint geometrical and mechanical properties be proposed? This kind of damage tensor is not only in good agreement with the failure mechanism of the jointed rock mass but also applicable to use, which can avoid the error in selecting the parameters to a large extent. Many scholars have done many works on it. For instance, Li et al. [23] obtained the calculation method of the damage tensor of the rock mass with nonpersistent joints based on the strain energy theory, which perfectly considers the joint geometrical and mechanical properties at the same time. It provides a good idea for studying the damage model for the rock mass with nonpersistent joints. So in view of it, the calculation method of the damage tensor which can consider both the joint geometrical and mechanical properties is set up based on the energy principle and facture mechanics. Then the corresponding damage constitutive model for the rock mass with nonpersistently closed joints under uniaxial compression is set up.

3.1 Establishment of the Damage Model for Rock Mass with Nonpersistently Closed Joints

According to fracture mechanics, for a planar stress problem under compression, the increment of the addition strain energy U_1 because of the existence of joints is:

$$U_1 = \int_0^A G \mathrm{d}A = \frac{1}{E} \int_0^A \left(K_{\mathrm{I}}^2 + K_{\mathrm{II}}^2 \right) \mathrm{d}A \tag{11}$$

where A is the joint area, K_{I} and K_{II} are the first and second stress intensity factors (SIF) of the joint tip, respectively, and E and G are Young's elastic modulus and shear modulus of the corresponding intact rock, respectively.

For a single joint, $A = Ba$ (unilateral joint) or $2Ba$ (centraljoint). For many joints, $A = NBa$ (unilateral joint) or $2NBa$ (central joint), where N is the joint number, B is the joint depth, and a is the joint half length.

Under the uniaxial stress σ, the emission of damaged strain energy Y is [24]:

$$Y = -\frac{\sigma^2}{2E(1-D)^2} \tag{12}$$

U^{E} is the unit volume elastic strain energy corresponding to the stress σ, and under the uniaxial stress condition, it can be expressed as [25]:

$$U^{\mathrm{E}} = -(1-D)Y \tag{13}$$

Substituting Eq. (12) into Eq. (13), we have:

$$U^{\mathrm{E}} = \frac{\sigma^2}{2E(1-D)} \tag{14}$$

When the rock mass does not contain any joints, $D = 0$, and Eq. (14) can be changed into:

$$U_0^{\mathrm{E}} = \frac{\sigma^2}{2E} \tag{15}$$

The increment of the unit volume elastic strain energy caused by the joints is:

$$\Delta U^{\mathrm{E}} = U^{\mathrm{E}} - U_0^{\mathrm{E}} = \frac{\sigma^2}{2E(1-D)} - \frac{\sigma^2}{2E} \tag{16}$$

Assuming the volume of the rock mass is V, the increment of the elastic strain energy caused by the joints is:

$$\Delta U^{\mathrm{E}} = V \left[\frac{\sigma^2}{2E\,(1-D)} - \frac{\sigma^2}{2E} \right] \tag{17}$$

Both ΔU^{E} in Eq. (17) and U_1 in Eq. (11) are the increment of the elastic strain energy caused by the joints, and they should be equal to each other:

$$\Delta U^{\mathrm{E}} = U_1 \tag{18}$$

or

$$\frac{1}{E} \int_0^A \left(K_{\mathrm{I}}^2 + K_{\mathrm{II}}^2 \right) \mathrm{d}A = V \left[\frac{\sigma^2}{2E(1-D)} - \frac{\sigma^2}{2E} \right] \tag{19}$$

From Eq. (19), we obtain:

$$D = 1 - \frac{1}{1 + \frac{2}{V\sigma^2}\int_0^A \left(K_{\mathrm{I}}^2 + K_{\mathrm{II}}^2\right) \mathrm{d}A} \tag{20}$$

Next, the SIF K_{I} and K_{II} are solved with the mechanical analysis of the jointed rock mass.

3.2 SIF Calculation Method

3.2.1 SIF Calculation Method of a Single Nonpersistently Closed Joint in Rock Mass

Under compression, the shear stress will make the rock mass have the trend of sliding along the joint face. Because of the closure of the joint, the direction of the friction force is opposite to that of the sliding. When the shear stress along the joint face exceeds the friction, the rock mass will slide along the joint face. With the increase in compression, the wing cracks will begin to propagate from the joint tips at the direction of 70.5° [26–28]; namely, the joints will propagate along the direction in which the tensile stress is maximum, as shown in Fig. 1. Then the wing cracks are formed.

Under the uniaxial compression, the normal and shear stresses on the joint face are as follows, respectively:

$$\sigma(\sigma, \alpha) = \frac{\sigma}{2} + \frac{\sigma}{2}\cos 2\alpha = \sigma\cos^2\alpha \tag{21}$$

$$\tau(\sigma, \alpha) = \frac{\sigma}{2}\sin 2\alpha \tag{22}$$

where $\sigma(\sigma, \alpha)$ and $\tau(\sigma, \alpha)$ are the normal and shear stresses on the joint face, respectively, α is the joint dip angle.

If assume the joint internal friction angle is φ, its friction coefficient μ is $\tan\varphi$. Then under the uniaxial compression, the shear stress on the joint face will cause the rock block to slide along it. In turn, the normal stress on the joint face will produce the friction force to resist the slippage of the rock block along it. So the slide force along the joint face τ_{eff} must be more than or equal to 0 and cannot be less than 0. Therefore, τ_{eff} can be obtained from Eqs. (21) and (22):

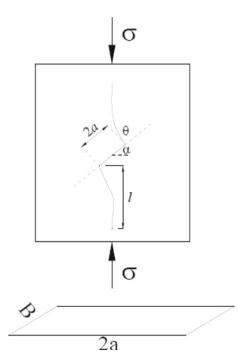

Fig. 1 Sketch of wing crack growth model. Joint length $2a$, joint dip angle α, growing crack length l, joint depth B

$$\tau_{\mathrm{eff}} = \begin{cases} 0 & \tan\alpha < \tan\varphi \\ \tau - \mu\sigma & \tan\alpha \geq \tan\varphi \end{cases} \tag{23}$$

It is noted that because the cohesion on the joint face is much less than friction force, it is neglected here.

The SIF K_{I} and K_{II} of the wing cracks at the joint tip can be revised as follows according to Lee [29] and the propagation direction of the wing cracks:

$$\begin{aligned} K_{\mathrm{I}} &= -\frac{2a\tau_{\mathrm{eff}}\sin\theta}{\sqrt{\pi(l+l^*)}} + p(\boldsymbol{\sigma}, \alpha+\theta)\sqrt{\pi l} \\ K_{\mathrm{II}} &= -\frac{2a\tau_{\mathrm{eff}}\cos\theta}{\sqrt{\pi(l+l^*)}} - \tau(\boldsymbol{\sigma}, \alpha+\theta)\sqrt{\pi l} \end{aligned} \tag{24}$$

where a is half length of the joint, and $l^* = 0.27a$ was introduced [30] to make K_{I} and K_{II} nonsingular when the tensile crack length is small. l is the propagation length of the wing cracks. θ is the propagation angle of the wing crack at the joint tip, and it is assumed to be 70.5° [26,27].

Considering the critical condition of the wing cracks to propagate, namely, $l = 0$, K_{I} and K_{II} of the wing cracks are:

$$\begin{aligned} K_{\mathrm{I}} &= -\frac{2a\tau_{\mathrm{eff}}\sin\theta}{\sqrt{\pi l^*}} \\ K_{\mathrm{II}} &= -\frac{2a\tau_{\mathrm{eff}}\cos\theta}{\sqrt{\pi l^*}} \end{aligned} \tag{25}$$

From the statement above, it is known that the critical condition that the wing crack length $l = 0$ is the initial condition that the nonpersistent joint begins to propagate. If the SIF of the joint tip at this moment is solved, the initial damage variable of the rock mass caused by the original nonpersistently closed joint can be obtained from Eq. (10). It is obviously seen that the damage obtained with this method includes not only the joint geometrical property such as its length and dip angle but also its mechanical one such as its internal friction angle. So the jointed rock mass damage constitutive model obtained from this method is more in agreement with the actual condition, and the joint transferring coefficients of compression and shear stresses are not required to revise it.

3.2.2 SIF Calculation Method of One or More Rows of Paralleled Nonpersistently Closed Joints in Rock Mass

If there is not one but a row of infinite nonpersistently closed joints with the same length and the same interval whose geometrical parameters are shown in Fig. 2, the effective SIF is by considering the interaction among the joints [31]:

$$\begin{aligned} K_{\mathrm{I}} &= K_{\mathrm{I0}}\sqrt{\frac{2}{\pi\phi}\tan\frac{\pi\phi}{2}} \\ K_{\mathrm{II}} &= K_{\mathrm{II0}}\sqrt{\frac{2}{\pi\phi}\tan\frac{\pi\phi}{2}} \end{aligned} \tag{26}$$

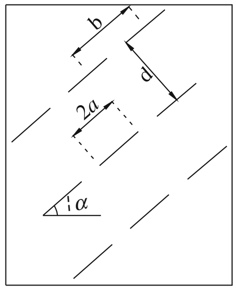

Fig. 2 Rock mass with nonpersistently closed joint. Joint length $2a$, joint dip angle α, joint center distance b, joint row interval d

Table 1 The value of $f(a, b, d)$

$d/2a$	$b/2a$				
	∞	5.0	2.5	1.67	1.25
∞	1.0	1.017	1.075	1.208	1.565
5	1.016	1.020	1.075	1.208	1.565
1	1.257	1.257	1.258	1.292	1.580
0.25	2.094	2.094	2.094	2.094	2.107

where K_{I0} and K_{II0} are SIF of one single I and II types of joints, respectively, K_I and K_{II} are SIF of many I and II types of joints, and ϕ is the persistent ratio of the nonpersistent joints, $\phi = \frac{2a}{b}$.

If the rock mass contains many rows of nonpersistently closed joints, the effective SIF is:

$$K_I = f(a, b, d)K_{I0}$$
$$K_{II} = f(a, b, d)K_{II0} \tag{27}$$

where $f(a, b, d)$ is the coefficient to reflect the interaction between joints, a, b, d are shown in Fig. 2.

The value of $f(a, b, d)$ is shown in Table 1 proposed by Cherepanov [32].

3.3 The Damage Variable of Rock Mass with One Set of Closed Joints

When the rock mass contains a set of one-rowed nonpersistently closed joints, it can be obtained by substituting Eq. (21)–(23) into (25)–(26) and (20):

$$D = \begin{cases} 0 & \tan\alpha < \tan\varphi \\ 1 - \frac{1}{1+\frac{12BNa^2}{V\phi}\tan\frac{\pi\phi}{2}\cos^2\alpha(\sin\alpha-\cos\alpha\tan\varphi)^2} & \tan\alpha \geq \tan\varphi \end{cases} \tag{28}$$

When the rock mass contains a set of more-rowed nonpersistently closed joints, it can be obtained by substituting Eq. (21)–(23) into (25), (27) and (20):

$$D = \begin{cases} 0 & \tan\alpha < \tan\varphi \\ 1 - \frac{1}{1+\frac{18.86BNa^2}{V}f^2(a,b,d)\cos^2\alpha(\sin\alpha-\cos\alpha\tan\varphi)^2} & \tan\alpha \geq \tan\varphi \end{cases} \tag{29}$$

where N is the joint number, V is the volume of the rock mass, and the other parameters are as above.

However, the damage caused by the joints to rock mass only denotes that along the loading direction. So it is necessary to make it tensorial in order to reflect the anisotropy of the macroscopic damage. Here the method proposed by Chen et al. [33] is adopted, and the following damage tensor $\mathbf{\Omega}$ is introduced:

$$\mathbf{\Omega} = \begin{bmatrix} D_0 & 0 & 0 \\ 0 & 0 & 0 \\ 0 & 0 & 0 \end{bmatrix} \tag{30}$$

where D_0 is the damage along the loading direction, which can be solved with Eq. (28) or (29).

4 A Damage Constitutive Model for Jointed Rock Mass by Coupling Macroscopic and Mesoscopic Flaws

4.1 The Damage Variable by Coupling Macroscopic and Mesoscopic Flaws

The damage variable of the jointed rock mass by considering the macroscopic and mesoscopic flaws is firstly discussed. The coupling of these two kinds of flaws is that of their corresponding damage variables [15].

In the calculation of coupled damage variable of these two kinds of flaws, the following hypotheses are adopted: ① The scale of macroscopic and mesoscopic flaws is differing in size of millimeters. The macroscopic flaws are assumed to be anisotropic, and the mesoscopic damage is isotropic. ② These two kinds of damages are described with different methods introduced in section 2 and 3, respectively. ③ The calculation method of the coupled damage variable follows Lemaitre strain equivalence hypothesis [34]. It states that the deformability of the damaged material can be calculated only with the effective stress. Its constitutive model can also be defined as the undamaged form, in which the stress σ should be replaced with the effective stress $\tilde{\sigma}$.

Under the stress, the damage strain caused by the coupled damage is the combination of these two kinds of damages, shown in Fig. 3. According to Lemaitre strain equivalence hypothesis, there is

$$\varepsilon_{12} = \varepsilon_1 + \varepsilon_2 - \varepsilon_0 \tag{31}$$

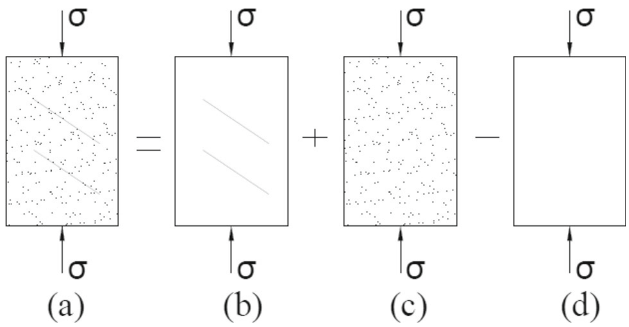

Fig. 3 Calculation of the equivalence strain. Parts **a–d** are the rock mass samples with both macroscopic and mesoscopic flaws, with only macroscopic flaws, with only mesoscopic flaws and without any flaws, respectively. Their elastic modulus and strain under stress σ are $\tilde{E}_{12}$, $\tilde{E}_1$, $\tilde{E}_2$, E_0 and ε_{12}, ε_1, ε_2, ε_0, respectively

in which the physical meaning of ε_{12}, ε_1, ε_2 and ε_0 is defined in Fig. 3.

Then we can obtain:

$$\frac{\sigma}{\tilde{E}_{12}} = \frac{\sigma}{\tilde{E}_1} + \frac{\sigma}{\tilde{E}_2} - \frac{\sigma}{\tilde{E}_0} \tag{32}$$

or

$$\frac{1}{\tilde{E}_{12}} = \frac{1}{\tilde{E}_1} + \frac{1}{\tilde{E}_2} - \frac{1}{\tilde{E}_0} \tag{33}$$

We assume the damage variables in the loading direction produced by the macroscopic and mesoscopic damages are D_1 and D_2, respectively, and their coupled damage variable is D_{12}. From Lemaitre strain equivalence hypothesis, it is known that:

$$\begin{cases} \tilde{E}_{12} = E_0 (1 - D_{12}) \\ \tilde{E}_1 = E_0 (1 - D_1) \\ \tilde{E}_2 = E_0 (1 - D_2) \end{cases} \tag{34}$$

Substituting Eq. (34) into Eq. (33), it obtains that:

$$D_{12} = 1 - \frac{(1 - D_1)(1 - D_2)}{1 - D_1 D_2} \tag{35}$$

Then the two extreme conditions are discussed following. First, when the rock mass contains only the macroscopic damage, namely $D_2 = 0$, we obtain $D_{12} = D_1$ from Eq. (35). It indicates that the coupled damage variable is equal to the macroscopic damage variable, and it agrees with the actual condition. If the rock mass contains only the mesoscopic damage, namely $D_1 = 0$, we have $D_{12} = D_2$, which indicates that the coupled damage variable is equal to the mesoscopic damage variable. It shows that the coupled damage variable obtained from the above method can apply to these two conditions.

Also based on Lemaitre strain equivalence hypothesis, the rock mass damage variable by coupling macroscopic and mesoscopic damages obtained by Yang et al. [15] was in Eq. (36).

$$D_{12} = 1 - \frac{(1 - D_1)(1 - D_2)}{(1 - D_1) + (1 - D_2)} \tag{36}$$

It can be seen from Eq. (36) that $D_{12} = \frac{1}{2 - D_2}$, namely $D_{12} \neq D_2$ when $D_1 = 0$. That is to say, when rock mass only contains mesoscopic damage, the coupled damage variable is not equal to the mesoscopic one, which is not obviously in agreement with the fact. From the deduction process of the coupling damage variable by Yang et al. [15], it can be found that it regarded that $\varepsilon_{12}$was the summation of ε_1 and ε_2. It calculated the strain caused by the rock mass without any damage twice; namely, it does not subtract the strain caused by the sample in Fig. 3d, and so its result is not rational.

If assume the damage tensor and variable caused by the macroscopic and mesoscopic flaws are $\mathbf{\Omega}$ or D, respectively, the coupled damage tensor $\mathbf{\Omega_{12}}$ can be expressed as:

$$\mathbf{\Omega_{12}} = \mathbf{I} - \frac{(\mathbf{I} - \mathbf{\Omega})(1 - D)}{\mathbf{I} - \mathbf{\Omega} D} \tag{37}$$

4.2 The Damage Constitutive Model for Rock Mass

Assuming the strength of the mesoscopic elements in rock blocks conforms to Weibull distribution and according to the damage theory, the jointed rock mass constitutive damage model by coupling the macroscopic and mesoscopic flaws is:

$$\{\sigma\} = [\mathbf{E_0}] \frac{(\mathbf{I} - \mathbf{\Omega})(1 - D)}{\mathbf{I} - \mathbf{\Omega} D} \{\boldsymbol{\varepsilon}\} \tag{38}$$

where $\mathbf{\Omega}$ and D are the second-order damage tensor and damage variable caused by the macroscopic and mesoscopic flaws, respectively, and $[\mathbf{E_0}]$ is the second-order elastic tensor of the intact rock.

5 Analysis of Calculation Examples

5.1 The Stress–Strain Diagram of Jointed Rock Mass

In order to validate the proposed model, the test done by Ling et al. [35] is adopted. The cylindrical sample is red sandstone with 50mm in diameter and 100mm in length. Its uniaxial compressive test diagram is shown in Fig. 4.

The Young's modulus E and Poisson's ratio ν of the red sandstone sample can be determined directly from the test data: $E = 6949$ MPa and $\nu = 0.22$. So the parameter m and

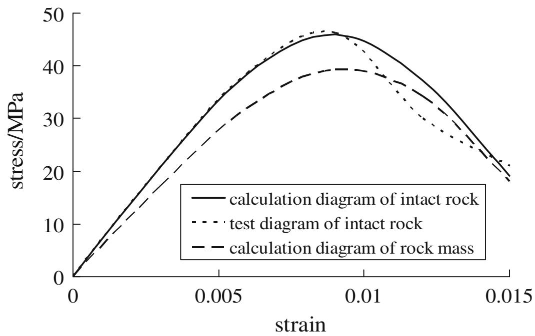

Fig. 4 Comparison between the test and theoretical diagrams

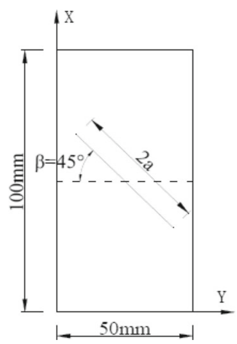

Fig. 5 The calculation model. Joint length $2a$, joint dip angle 45°

ε_0 of the rock sample can be obtained with Eq. (8): $m = 3.3352$ and $\varepsilon_0 = 0.0128$.

Theoretical compressive stress–strain diagram from the constitutive model with only mesoscopic flaws can be obtained by substituting the distribution parameters and stress–strain diagram test data into Eq. (7), which fits well with the test diagram (Fig. 4).

Assume there is a nonpersistently closed joint in the sample (Fig. 5), and the joint depth, length, dip angle and internal friction angle are 1, 4 cm, 45° and 15° (ignoring its cohesion), respectively. The macroscopic damage tensor $\boldsymbol{\Omega}$ along the loading direction caused by the joint according to the calculation method proposed in this paper is $\boldsymbol{\Omega} = \begin{bmatrix} 0.17 & 0 & 0 \\ 0 & 0 & 0 \\ 0 & 0 & 0 \end{bmatrix}$.

For a planar stress problem under compression, the damage constitutive model for jointed rock mass can be obtained according to Eq. (38). Then the theoretical stress–strain diagram of jointed rock mass is shown in Fig. 4. It can be seen that: ① When the rock mass contains only mesoscopic damage, the mesoscopic damage model based on Weibull distribution can perfectly reflect the stress–strain relationship of the rock. The theoretical diagram fits very well with the test one, especially before the peak strength. ② However, when the rock mass contains the macroscopic flaw namely the joint, its mechanical behavior will be evidently intenerated. For this calculation example, the peak strength of the rock mass with a nonpersistently closed joint is 39.41 MPa, 85.8 % of the intact rock. These results show that the rock mass strength and stiffness are weakened by the joint. ③ From the characteristic of the sample's stress–strain diagram, one of the rock mass with these two kinds of flaws differs from that of the rock mass with only the mesoscopic flaws very much before the peak strength, and then the gap between them gradually becomes less and less. Finally their residual strength is nearly the same.

5.2 The Mechanical Behaviors of Rock Mass with Different Joint Dip Angle

Here the calculation model in Fig. 5 is adopted to discuss the effect law of joint dip angle β on the sample's stress–strain diagram. It can be seen from Fig. 6 that: ① For the rock mass with a joint of different dip angle, their stress–strain diagrams are basically the same, but their peak strength is different. For values of β, between 0 and 15°(φ) or very close to 90°, no sliding occurs on the planes of the joint, and the samples' climax strengthes are the same. This is because the sample's strength depends on shear failure or axial splitting of intact rock in a direction not controlled by the joint. The minimum strength appears for a joint dip 52.5°($45^0 + \varphi/2$), which fits with the existing research conclusions [36]. ② It can be seen from change amplitude of the sample's peak strength that the peak strength of the sample with a joint dip 52.5° is 39.03 MPa, 85.5 % of that of the samples with a joint dip 0° or 90°. It indicates that the joint dip angle has effect on the sample's mechanical behaviors.

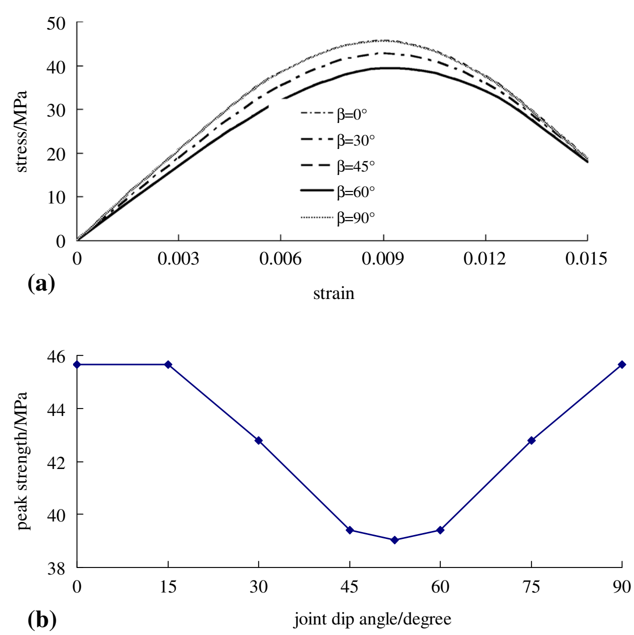

Fig. 6 The mechanical behaviors of the samples with different joint dip angle. **a** Stress-strain diagrams. **b** Change law of the sample's uniaxial compressive peak strength with joint dip angle

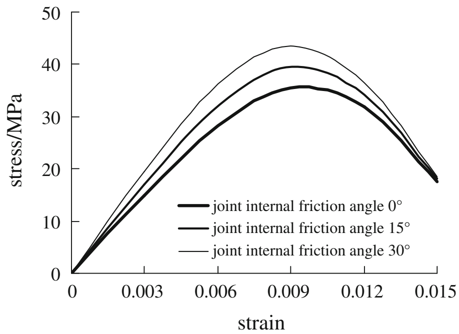

Fig. 7 The stress–strain diagrams of the samples with different joint internal friction angle under uniaxial compression

5.3 The Mechanical Behaviors of Rock Mass with Different Joint Internal Friction Angle

Here the calculation model in Fig. 5 is still adopted. The joint dip angle and its length are 45° and 4 cm, respectively. Assume the joint internal friction angle is 0°, 15° and 30°, respectively. It can be seen from Fig. 7 that the slope of the rock mass stress–strain diagrams increases with the joint internal friction angle, which indicates that the rock mass elastic modulus increases with the joint internal friction angle. Meanwhile, the rock mass peak strength increases with the joint internal friction angle, and this is because the joint shear strength increases with the joint internal friction angle, and accordingly the damage caused by the joint to the rock mass decreases, and the rock mass strength increases. It indicates that the joint shear strength has effect on the rock mass mechanical behaviors such as stress–strain diagram and peak strength.

5.4 The Mechanical Behaviors of Rock Mass with Different Joint Length

Here the calculation model in Fig. 5 is still adopted. The joint dip angle and internal friction angle are 45° and 15°, respectively. Assume the joint length is 1, 2, 3 and 4 cm, respectively. It can be seen from Fig. 8 that the slope of the rock mass stress–strain diagrams decreases with the joint length, which indicates that the rock mass elastic modulus decreases with the joint length. This is because the damage caused by the joint to the rock mass increases with the joint length, and accordingly the rock mass strength decreases. Meanwhile, it can be seen from Fig. 8b that the sample's peak strength decreases almost linearly with the joint length. When the joint length increases from 1 to 4 cm, the sample's peak strength decreases from 45.3 to 39.41 MPa, whose amplitude is about 13.0 %. It indicates that the joint length has effect on the rock mass mechanical behaviors such as stress–strain diagram and peak strength.

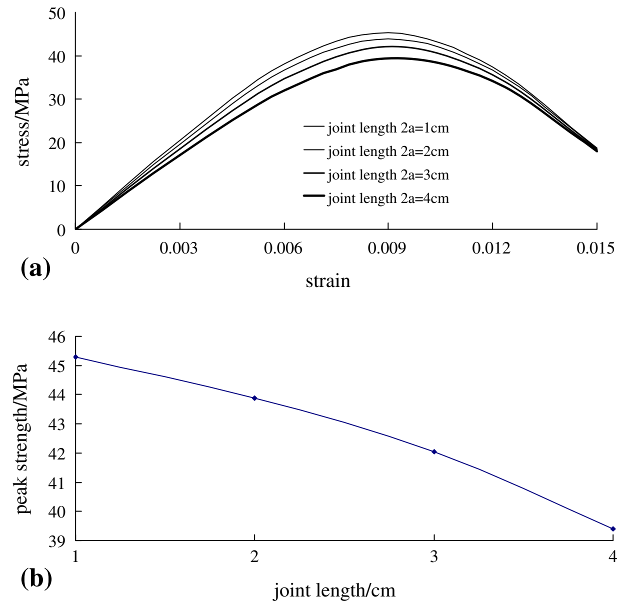

Fig. 8 The mechanical behaviors of the samples with different joint length under uniaxial compression. **a** Stress-strain diagrams. **b** Change law of the sample's uniaxial compressive peak strength with joint length

6 Conclusions

In this study, rock mass is assumed to be a compound damage material, and then we investigate the effect of the macroscopic and mesoscopic flaws on its mechanical behavior. The damage caused by the mesoscopic flaws is described by the damage constitutive model based on Weibull distribution. Based on the energy principle and fracture mechanics, we propose the calculation method of the macroscopic damage tensor caused by the joints, which can consider the effect of the joint geometrical and mechanical property on the rock mass mechanical behaviors.

On the basis of Lemaitre strain equivalence hypothesis, the coupled damage variable is deduced. Then the damage constitutive model for jointed rock mass under uniaxial compression by coupling the macroscopic and mesoscopic flaws is set up. Next, the proposed model is validated with the test data.

Finally, the proposed model is adopted to discuss the effect of joint dip angle, joint internal friction angle and joint length on the mechanical behavior of rock mass with one single nonpersistently closed joint. Overall, the proposed model provides a way to simulate on how the macroscopic and mesoscopic flaws affect the mechanical behavior of rock mass with nonpersistently closed joints.

Acknowledgments This study is supported by the Fundamental Research Funds for the Central Universities of China (Grant No. 2-9-2014-019), the Ministry of Education Science and Technology Key Research

Funds of China (Grant No. 211175) and the National natural science Foundation of China (Grant Nos. 41002113, 41162009).

References

1. Wang, T.T.; Huang, T.H.: A constitutive model for the deformation of a rock mass containing sets of ubiquitous joints. Int. J. Rock Mech. Min. Sci. **46**, 521–530 (2009)
2. Halakatevakis, N.; Sofianos, A.L.: Strength of a blocky rock mass based on an extended plane of weakness theory. Int. J. Rock Mech. Min. Sci. **47**, 568–582 (2010)
3. Prudencio, M.; Van Sint Jan, M.: Strength and failure modes of rock mass models with non-persistent joints. Int. J. Rock Mech. Min. Sci. **44**, 890–902 (2007)
4. Verma, A.K.; Singh, T.N.: Modeling of a jointed rock mass under triaxial conditions. Arab. J. Geosci. **3**, 91–103 (2010)
5. Wang, T.T.; Huang, T.H.: Anisotropic deformation of a circular tunnel excavated in a rock mass containing sets of ubiquitous joints: theory analysis and numerical modeling. Rock Mech. Rock Eng. **47**, 643–657 (2014)
6. Wai, L.C.; Asadul, H.; Ranjith, P.G.; Akm, S.: Modelling of intact and jointed mudstone samples under uniaxial and triaxial compression. Arab. J. Geosci. **6**, 1639–1646 (2013)
7. Ramamurthy, T.; Arora, V.K.: Strength predictions for jointed rocks in confined and unconfined states. Int. J. Rock Mech. Min. Sci. **31**, 9–22 (1994)
8. Tang, C.A.; Liu, H.; Lee, P.K.K.; Tsui, Y.; Tham, L.G.: Numerical studies of the influence of microstructure on rock failure in uniaxial compression—Part I: effect of heterogeneity. Int. J. Rock Mech. Min. Sci. **37**, 555–569 (2000)
9. Xie, N.; Zhu, Q.Z.; Xu, L.H.; Shao, J.F.: A micromechanics-based elastoplastic damage model for quasi-brittle rocks. Comput. Geotech. **38**, 970–977 (2011)
10. Kawamoto, T.; Ichikawa, Y.; Kyoya, T.: Deformation and fracturing behavior of discontinuous rock mass and damage mechanics theory. Int. J. Numer. Anal. Met. **12**, 1–30 (1988)
11. Swoboda, G.; Shen, X.P.; Rosas, L.: Damage model for jointed rock mass and its application to tunneling. Comput. Geotech. **22**, 183–203 (1998)
12. Grady, D.E.; Kipp, M.E.: The micromechanics of impact fracture of rock. Int. J. Rock Mech. Min. Sci. **16**, 293–302 (1979)
13. Taylor, L.M.; Chen, E.P.; Kuszmaul, J.S.: Microcrack induced damage accumulation in brittle rock under dynamic loading. Comput. Meth. Appl. Mech. Eng. **55**, 301–320 (1986)
14. Niu, S.J.; Jing, H.W.; Hu, K.; Yang, D.F.: Numerical investigation on the sensitivity of jointed rock mass strength to various factors. Min. Sci. Tech. **20**, 530–534 (2010)
15. Yang, G.S.; Xie, D.Y.: Coupling Analysis on the Macro-damage and Meso-damage of Rock Masses: Symposium on the Sixth National Rock Mechanics and Engineering Academic Conference, pp. 327–329, Wuhan (2000); (in Chinese)
16. Krajcinovic, D.; Silva, M.A.G.: Statistical aspects of the continuous damage theory. Int. J. Solids Struct. **18**, 555–562 (1982)
17. Wang, Z.L.; Li, Y.C.; Wang, J.G.: A damage-softening statistical constitutive model considering rock residual strength. Comput. Geosci. **33**, 1–9 (2007)
18. Weibull, W.: A statistical distribution function of wide applicability. J. Appl. Mech. **18**, 293–297 (1951)
19. Goodman, R.E.; Taylor, R.E.; Brekke, T.: A model for the mechanics of jointed rock. ASCE J. Soil Mech. Found Div. **94**, 637–659 (1986)
20. Desai, C.S.; Zaman, M.M.; Lightner, J.G.; Siriwardane, H.J.: Thin-layer element for interfaces and joints. Int. J. Numer. Meth. Geomech. **8**, 19–43 (1984)
21. Zhao, D.; Swoboda, G.; Laabmayr, F.: Damage mechanics and its application for the design of an underground theater. Tunn. Undergr. Sp. Tech. **19**, 567–575 (2004)
22. Liu, T.Y.; Cao, P.; Lin, H.: Evolution procedure of multiple rock cracks under seepage pressure. Math. Probl. Eng. **5**, 1–11 (2013)
23. Li, N.; Chen, W.; Zhang, P.: The mechanical properties and a fatigue-damage model for jointed rock mass subjected to dynamic cyclical loading. Int. J. Rock Mech. Min. Sci. **38**, 1071–1079 (2001)
24. Lou, Z.W.: Fundamental of Damage Mechanics. Xi'an Jiaotong University Press, Xi'an (1991); (in Chinese)
25. Liu, X.M.; Li, Z.F.: Damage mechanics analysis for brittle rock and rockburst energy index. Chin. J. Rock Mech. Eng. **16**, 140–147 (1997); (in Chinese)
26. Huang, C.; Subhash, G.; Vitton, S.J.: A dynamic damage growth model for uniaxial compressive response of rock aggregates. Mech. Mater. **34**, 267–277 (2002)
27. Huang, C.; Subhash, G.: Influence of lateral confinement on dynamic damage evolution during uniaxial compressive response of brittle solids. J. Mech. Phys. Solid **51**, 1089–1105 (2003)
28. Paliwal, B.; Ramesh, K.T.: An interacting micro-crack damage model for failure of brittle materials under compression. J. Mech. Phys. Solid **56**, 896–923 (2008)
29. Lee, S.; Ravichandran, G.: Crack initiation in brittle solids under multiaxial compression. Eng. Fract. Mech. **70**, 1645–1658 (2003)
30. Horii, H.; Nemat-Nasser, S.: Brittle failure in compression: splitting, faulting and brittle–ductile transition. Philos. Trans. R. Soc. Lond. **319**, 337–374 (1986)
31. Li, J.L.; Ha, Q.L.: A study of tensile-shear crack and strength related to jointed rock mass. Chin. J. Rock Mech. Eng. **17**, 259–266 (1998); (in Chinese)
32. Cherepanov, G.P.: Mechanics of Brittle Fracture. McGraw-Hill, New York (1977)
33. Chen, W.; Christian, L.B.; Olivier, M.; et al.: Simulation of damage-permeability coupling for mortar under dynamic loads. Int. J. Numer. Anal. Meth. Geomech. **38**, 457–474 (2014)
34. Lemaitre, J.: Evaluation of dissipation and damage on metals submitted to dynamic loading. In: Proceedings of ICM-1, Kyoto (1971)
35. Ling, J.M.; Sun, J.: On mesocrack damage of brittle rocks and its time-dependent characteristics. Chin. J. Rock Mech. Eng. **12**, 304–312 (1993); (in Chinese)
36. Jaeger, J.C.: Shear failure of anisotropic rocks. Geol. Mag. **97**, 65–79 (1960)